Circularly Polarized Stacked Annular-Ring Microstrip Antenna With Integrated Feeding Network for UHF RFID Readers

Xi Chen, Guang Fu, Shu-Xi Gong, Ya-Li Yan, and Wei Zhao

***Abstract*—A novel circularly polarized (CP) annular-ring microstrip antenna (ARMSA) is proposed for American ultrahigh frequency (UHF) radio frequency identification (RFID) readers. The annular ring is fed by an equal-split power divider with 90° phase difference. For the compactness of the entire antenna, the divider with the shape of Archimedes gradual-change lines is designed at the inside of the annular ring. A circular parasitic patch is suspended above the ring to improve the impedance matching and bandwidth. It also enhances the performances of axial ratio (AR). The impedance bandwidth for $S_{11} < -10$ dB and 3-dB AR bandwidth are 870–967 MHz (10.6% at 915 MHz) and 893–948 MHz (6%), respectively. The CP gain is 8.9 dBi at 915 MHz with the front-to-back ratio (F/B) of 16.5 dB. The proposed antenna is low profile as the total height is $0.043\lambda_0$ (λ_0 is the free-space wavelength).**

***Index Terms*—Annular-ring, axial ratio (AR), circularly polarized (CP), feeding network, microstrip antenna.**

I. Introduction

CIRCULARLY polarized (CP) microstrip antenna has been widely used in satellite communication, global positioning system (GPS), and radio frequency identification (RFID). Rectangular and circular patch microstrip antennas are traditionally applied to implement circular polarization [1], [2]. In recent years, annular-ring microstrip antenna (ARMSA) is becoming another available candidate. It can be achieved by cutting a concentric circular slot on a circular radiating patch. At a fixed operating frequency, an annular-ring patch can maintain similar radiation characters with a smaller dimension compared to that of a circular patch; it is mainly because the behavior of slotting on the patch extends the flowing path of the surface current [3]. The CP operation of the annular ring also involves introducing perturbation segments [4], [5] or adding CP feeding network [6], [7]. However, the very large input impedance of ARMSA is an obstacle when the annular ring works in TM_{11} and TM_{21} modes [8].

Some techniques have been reported to solve the problem. In [4], the authors adopt microstrip line as an impedance transformer to realize impedance matching with 50 Ω, and the transmission loss caused by the very narrow microstrip line has to be considered carefully. In [5] and [9], the coupling feeding is applied to improve the impedance matching. The approaches above hardly provide wide impedance and axial ratio (AR) bandwidths because of the single resonant mode. Stacking a parasitic patch above the annular ring can reduce the value of input impedance greatly, and the bandwidth can be broadened obviously due to the excitation of two adjacent resonant modes [7], [10].

In this letter, we propose a novel CP ARMSA. The circular polarization is produced by an equal-split power divider, which is reshaped and arranged at the inside of the annular ring for compactness. A stacked parasitic circular patch is used to improve the performances of impedance and AR. The effect of ground plane size is also studied for the consideration of small external dimensions and good antenna performances.

II. Antenna Design

The configuration of the proposed antenna is shown in Fig. 1(a). It only contains three components: a printed circuit broad (PCB) with an annular ring and a feeding network etched on it, a circular parasitic patch, and a square metallic ground. The PCB is a circular substrate with radius $R_s = 55$ mm ($0.168\lambda_0$ at 915 MHz, λ_0 is the free-space wavelength), thickness $t_s = 1$ mm ($0.003\lambda_0$), and relative permittivity $\varepsilon_r = 2.65$. The annular-ring patch is etched on it. The inner radius a and outer radius b of the ring are determined by the operating frequency. When the ring is designed to work in TM_{11} mode, the resonant frequency can be expressed as [5]

$$f_{11} = \frac{c}{\pi(a'+b')\sqrt{\varepsilon_{\mathrm{eff}}}} \tag{1}$$

where c represents the speed of light in free space, a' and b' represent respectively the inner and outer radius considering the fringing effect, and $\varepsilon_{\mathrm{eff}}$ represents the effective permittivity around the ring. $\pi(a'+b')$ can be seen as the mean circumferential length of the annular ring. From (1), there is

$$\pi(a'+b') = \frac{c}{f_{11}\cdot\sqrt{\varepsilon_{\mathrm{eff}}}} = \frac{\lambda_{11}}{\sqrt{\varepsilon_{\mathrm{eff}}}} \tag{2}$$

so the mean circumferential length of the ring is approximately the guided wavelength in effective permittivity. Some literature has reported the uses for the inner space of the ring. [4] arranges the meandered impedance transformer lines at the inside of the ring. [7] integrates a 3-dB branch-line coupler in an annular ring of TM_{21} mode, but the mean circumferential length of the ring is approximately twice the guided wavelength in effective permittivity. In our application, it is unsuitable to arrange a traditional divider in the annular ring of TM_{11} mode, so a reshaped equal-split power divider is designed and etched at the inside of the ring. To obtain the reduction of the divider size and

Manuscript received April 07, 2010; revised May 03, 2010; accepted May 25, 2010. Date of publication June 07, 2010; date of current version June 14, 2010.

The authors are with the National Key Laboratory of Antenna and Microwave Technology, Xidian University, Xi'an 710071, China (e-mail: chenxi1223@gmail.com; gfu@mail.xidian.edu.cn; shxgong@xidian.edu.cn)

Digital Object Identifier 10.1109/LAWP.2010.2051791

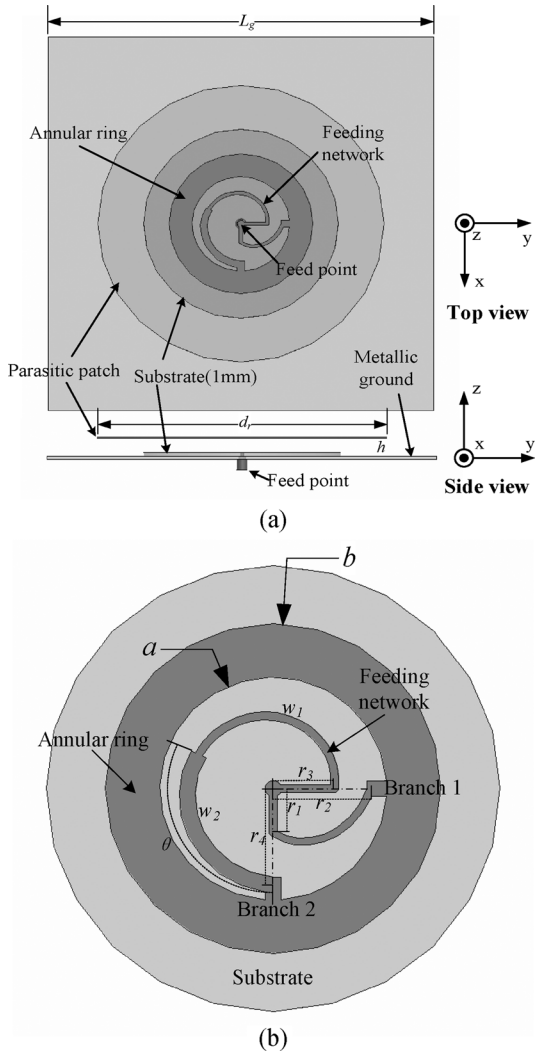

Fig. 1. Configurations of the proposed antenna. (a) Full view. (b) Local view. $a = 25.8$ mm, $b = 42.6$ mm, $d_{\rm r} = 167.9$ mm ($0.51\lambda_0$), $h = 10$ mm ($0.03\lambda_0$), $r_1 = 17$ mm, $r_2 = 22$ mm, $r_3 = 17$ mm, $r_4 = 25$ mm, $w_1 = 1.3$ mm, $w_2 = 2.4$ mm, $\theta = 120°$, and $L_{\rm g} = 220$ mm ($0.67\lambda_0$).

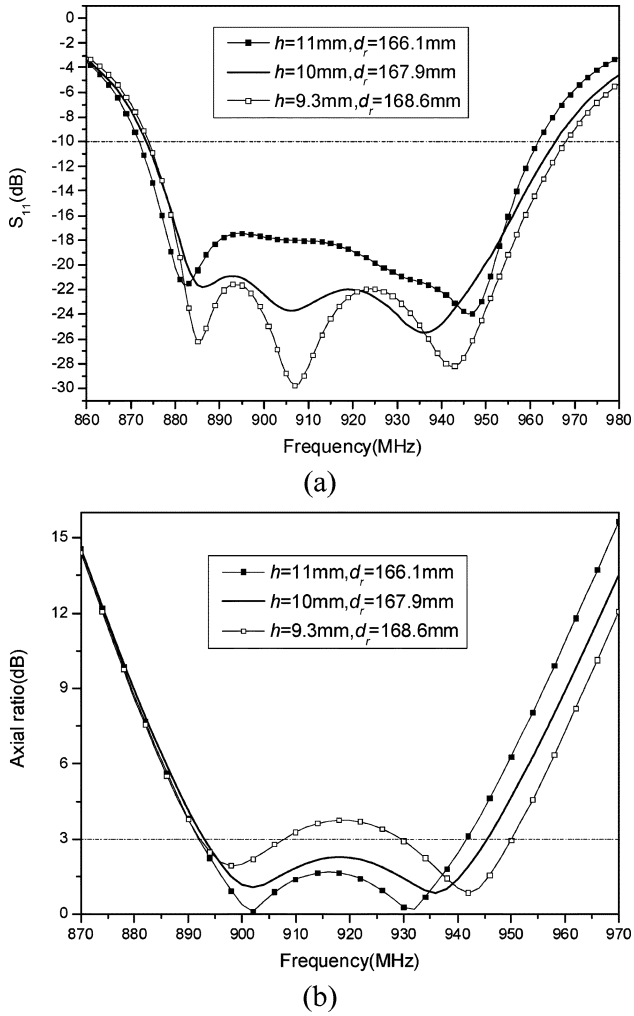

Fig. 2. S_{11} and AR of the proposed antenna with three groups of h and $d_{\rm r}$. (a) S_{11}. (b) AR.

the smoothness of the branch lines, Archimedes gradual-change lines are used to construct the branch lines of the divider.

Fig. 1(b) shows the local view of the feeding network and the annular ring. The principle of the network is identical with that of the traditional divider except the shapes. The length of Branch 1 is approximately $\lambda_{\rm g}/4$ and is controlled by r_1 and r_2, where $\lambda_{\rm g}$ is the guided wavelength; the length of Branch 2 is approximately $\lambda_{\rm g}/2$ and is controlled by r_3 and r_4. The segment adjusting 90°-phase shift is controlled by its corresponding central angle θ. The widths w_1 and w_2 of the microstrip lines determine their characteristic impedances of 70 Ω and 50 Ω, respectively. The final designing sizes are listed below Fig. 1. As is well known, introducing CP feeding network can provide wider bandwidths of impedance and AR, but a large insertion loss will lead to low radiation efficiency [6]. In this application, the isolation resistor is omitted, so the insertion loss of the network is very small and the radiation characters are well maintained.

To improve the impedance matching and bandwidth of the annular ring, we suspended a 0.8-mm-thickn circular parasitic patch above the PCB at the height h. When the diameter $d_{\rm r}$ of the patch is about a half-wavelength in free space, a good radiation feature can be obtained. Fig. 2 shows the S_{11} and AR curves of the proposed antenna with the different groups of h and $d_{\rm r}$. It indicates the antenna has the feature of double resonant modes, and as h decreases and $d_{\rm r}$ increases, the bandwidths of impedance and AR are both broadened. When $h = 11$ mm and $d_{\rm r} = 166.1$ mm, the AR values are lowest and its bandwidth is narrowest; when $h = 9.3$ mm and $d_{\rm r} = 168.6$ mm, the AR values are partially over 3 dB. A good compromise between lower AR values and wider AR bandwidth can be obtained by $h = 10$ mm and $d_{\rm r} = 167.9$ mm. The obvious effect comes from the strong electromagnetic (EM) mutual coupling between the ARMSA and the parasitic patch. According to the theoretical analysis in [7], the mutual coupling can be express as

$$M_{\rm c} = k_{\rm c}\sqrt{L_{\rm a} \cdot L_{\rm p}} \tag{3}$$

$$k_{\rm c} = \frac{f_2 - f_1}{f_0} = \frac{\Delta f}{f_0} \tag{4}$$

$$f_0 = \frac{f_2 + f_1}{2} \tag{5}$$

where $k_{\rm c}$ is a coupling coefficient of the two resonant modes, and $L_{\rm a}$ and $L_{\rm p}$ are self-inductances of the ARMSA and the parasitic patch, respectively. It can be explained that as the para-

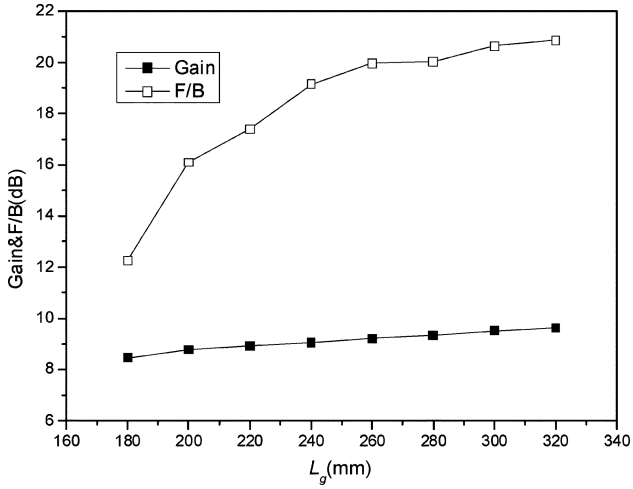

Fig. 3. Simulated CP gain and F/B versus ground side length L_g.

sitic patch approaches the annular ring, the enhancement of mutual coupling M_c will broaden the bandwidth Δf. However, the target values of the concerned electrical performances also have to be considered.

The square metallic ground is attached to the bottom surface of the substrate. The ground size is studied for a suitable choice. Fig. 3 shows the curves of the simulated CP gain and the front-to-back ratio (F/B) versus the ground side length L_g from 180 ($0.55\lambda_0$) to 320 mm ($0.98\lambda_0$) by 20-mm steps. The increase of L_g is beneficial to both the gain and the F/B. The gain rises flatly and uniformly, while the F/B rises rapidly before 240 mm and tends to be slow after that. Therefore, for better radiation performances and smaller total antenna dimensions, it is suitable to decide L_g in the range of 200–240 mm. Fig. 4 shows the simulated S_{11} and AR curves of the proposed antenna with different L_g. The impedance bandwidth for $S_{11} < -10$ dB is almost unchangeable, and the 3-dB AR bandwidth is also maintained well except at 180 mm. In practice, we choose 220 mm ($0.67\lambda_0$) as the designing size for calculations and experiments. Of course, a smaller ground size can be chosen for miniature ones if the adjustment of other parameters is provided.

III. Experimental Results and Discussion

To confirm the theoretical results, we fabricated prototypes with $h = 10$ mm, $d_r = 167.9$ mm, and $L_g = 220$ mm. The total external dimensions are $14 \times 220 \times 220$ mm^3 ($0.043\lambda_0 \times 0.67\lambda_0 \times 0.67\lambda_0$), so a low profile is still maintained compared to some RFID reader antennas [11]. Fig. 5 shows the measured S_{11} compared to simulated values. The measured impedance bandwidth for $S_{11} < -10$ dB is 870–967 MHz (10.6% at 915 MHz), and it agrees well with the simulated one. The difference between the measured values and the simulated ones is mainly due to the manufacture tolerances, e.g., the state of the soldering can cause a few changes to the input impedance.

Fig. 6 shows the measured CP gain and AR of the proposed antenna compared to the simulated results at broadside direction. The measured values of AR, CP gain, and the radiation patterns (RP) are all obtained through phase-amplitude method. From the figure, the measured 3-dB AR bandwidth is 893–948 MHz (6% at 915 MHz), and the values slightly

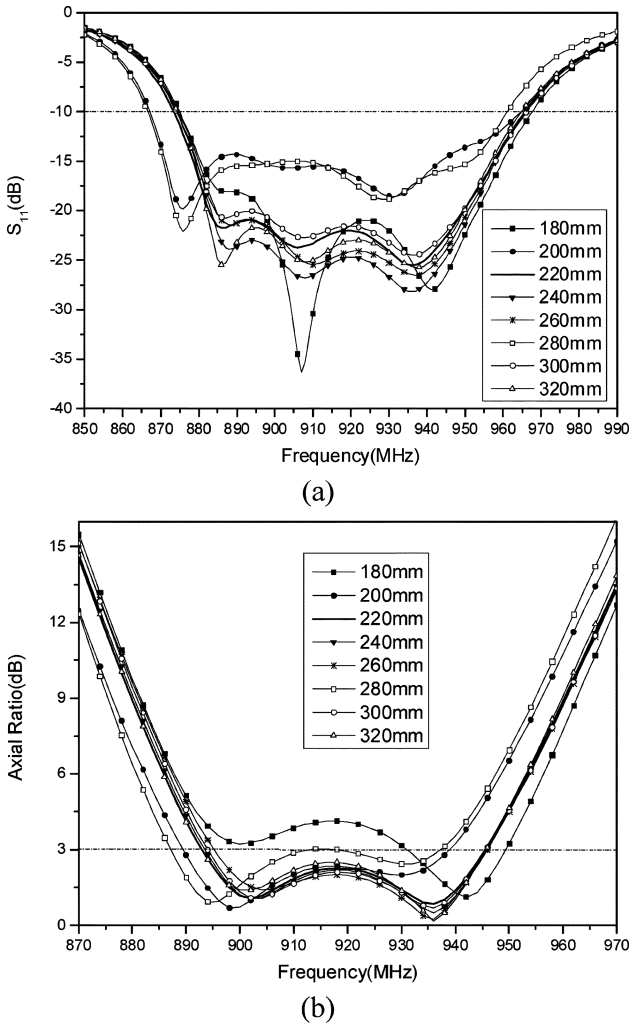

Fig. 4. Simulated S_{11} and AR of the proposed antenna with different ground sizes. (a) S_{11}. (b) AR.

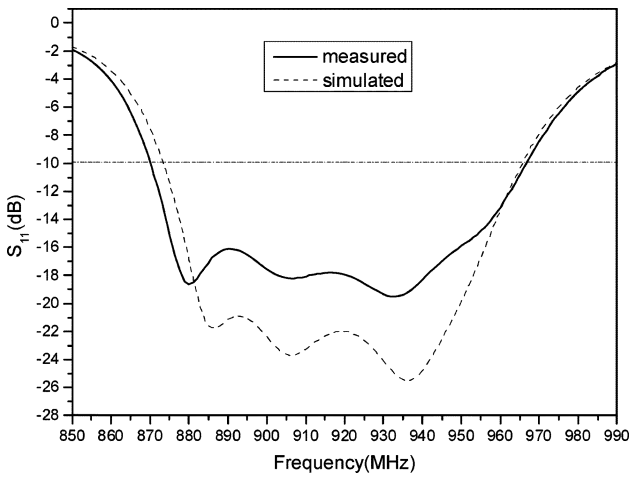

Fig. 5. Measured and simulated S_{11} of the proposed antenna.

shift toward higher frequency compared to the simulated one. The CP gain in this band also agrees with the simulated values despite some disturbances, which come from the measuring errors. The gain of 8.9 dBi is obtained at 915 MHz, and the gain is more than 8.5 dBi from 893 to 948 MHz. Therefore,

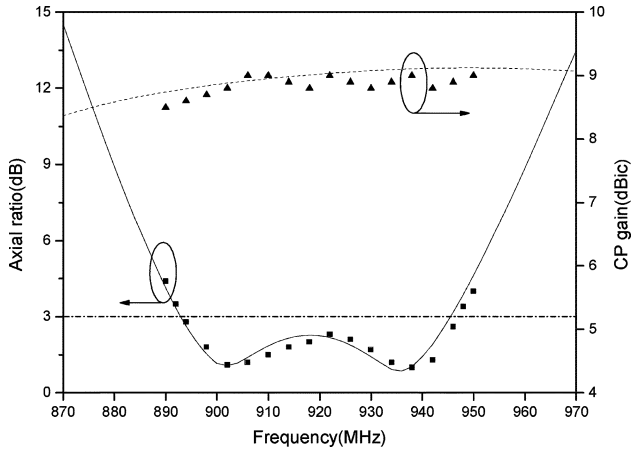

Fig. 6. Measured and simulated AR and CP gain. ——— Simulated AR, ■ measured AR, – – – Simulated CP gain, ▲ measured CP gain.

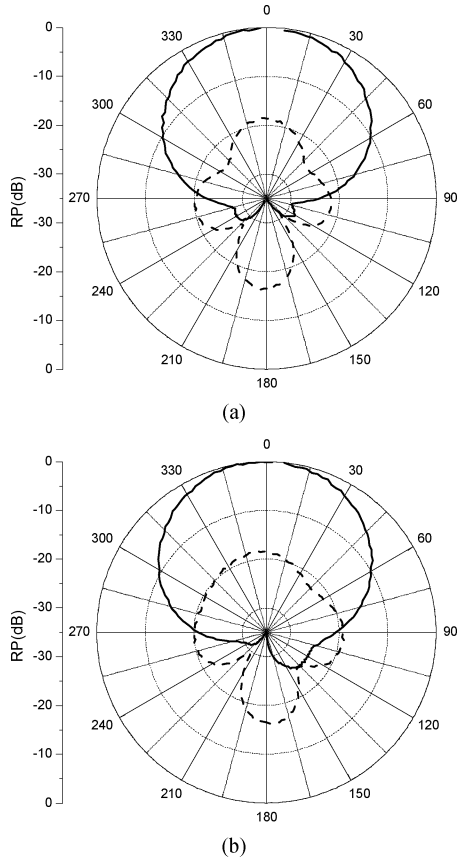

Fig. 7. Measured RP at 915 MHz. (a) At xz plane. (b) At yz plane. ——— LHCP pattern; – – – RHCP pattern.

the proposed antenna has better radiation performances and smaller ground electrical sizes than those of recent applications [6], [9], and [11].

The measured left-hand circular polarization (LHCP) and right-hand circular polarization (RHCP) RP at 915 MHz are shown in Fig. 7. The half-power beamwidth (HPBW) is 65° and 67°, respectively, in xz plane and yz plane. Obviously, a good symmetrical radiation behavior is acquired; it is mainly because the feeding network is integrated in the ring and does not destroy the symmetry of the entire antenna. Due to the suitable ground size, the F/B reaches 16.5 dB. It is predicted that the F/B will be enhanced further if the ground size increases.

IV. Conclusion

A novel CP stacked annular-ring microstrip antenna is proposed in this letter for UHF RFID application. The antenna contains an equal-split power divider, which is reshaped and arranged at the inside of the ring for compactness of the entire antenna. The parasitic patch above the annular ring can improve the bandwidths of impedance and AR obviously because two adjacent resonant modes are caused simultaneously. Furthermore, through experimental and theoretical analysis, we find the parameters of the parasitic patch have a sensitive effect on the values and bandwidth of AR. The experimental results indicate the impedance bandwidth for $S_{11} < -10$ and 3 dB AR bandwidth are 870–967 (10.6%) and 893–948 MHz (6%), respectively. The overlapped bandwidth can well cover American UHF RFID band and others. High CP gain of 8.9 dBi and good F/B of 16.5 dB is acquired respectively at 915 MHz due to the optimized ground size.

Acknowledgment

The authors would like to thank Mr. J.-L. Zhang for antenna fabrication, and the reviewers for helpful suggestions.

References

[1] Nasimuddin, K. P. Esselle, and A. K. Verma, "Wideband circularly polarized stacked microstrip antennas," *IEEE Antennas Wireless Propag. Lett.*, vol. 6, pp. 21–24, 2007.

[2] F. Ferrero, C. Luxey, G. Jacquemod, and R. Staraj, "Dual-band circularly polarized microstrip antenna for satellite applications," *IEEE Antennas Wireless Propag. Lett.*, vol. 4, pp. 13–15, 2005.

[3] Y. S. Wu and F. J. Rosenbaum, "Mode chart for microstrip ring resonators," *IEEE Trans. Microw. Theory Tech.*, vol. MTT-21, no. 7, pp. 487–489, Jul. 1973.

[4] H. M. Chen and K. L. Wong, "On the circular polarization operation of annular-ring microstrip antennas," *IEEE Trans. Antennas Propag.*, vol. 47, no. 8, pp. 1289–1292, Aug. 1999.

[5] Y. F. Lin, H. M. Chen, and S. C. Lin, "A new coupling mechanism for circularly polarized annular-ring patch antenna," *IEEE Trans. Antennas Propag.*, vol. 56, no. 1, pp. 11–16, Jan. 2008.

[6] Y. X. Guo, L. Bian, and X. Q. Shi, "Broadband circularly polarized annular-ring microstrip antenna," *IEEE Trans. Antennas Propag.*, vol. 57, no. 8, pp. 2474–2477, Aug. 2009.

[7] H. Ohmine, Y. Sunahara, and M. Matsunaga, "An annular-ring microstrip antenna fed by a co-planar feed circuit for mobile satellite communication use," *IEEE Trans. Antennas Propag.*, vol. 45, no. 6, pp. 1001–1008, Jun. 1997.

[8] W. C. Chew, "A broad-band annular-ring microstrip antenna," *IEEE Trans. Antennas Propag.*, vol. AP-30, no. 5, pp. 918–922, May 1982.

[9] K. F. Tong and J. J. Huang, "New proximity coupled feeding method for reconfigurable circularly polarized microstrip ring antennas," *IEEE Trans. Antennas Propag.*, vol. 56, no. 7, pp. 1860–1866, Jul. 2008.

[10] S. H. Al-Charchafchi, W. K. Wan Ali, and S. Sinkeree, "A stacked annular-ring microstrip patch antenna," in *IEEE APS Int. Symp. Dig.*, 1997, vol. 2, pp. 948–951.

[11] Z. N. Chen, X. M. Qing, and H. L. Chung, "A universal UHF RFID reader antenna," *IEEE Trans. Microw. Theory Tech.*, vol. 57, no. 5, pp. 1275–1282, May 2009.